# Advanced Machining Toolpath for Low Distortion

**FINAL STATUS REPORT**

**Prepared by**

Brian Becker
R&D Technology Manager
Third Wave Systems, Inc.
Minneapolis, MN
(952) 832-5515

for the

## U.S. Army - Aviation Development Directorate

Contract No: W911W6-16-P-0044

Contractor: Third Wave Systems, Inc.

Contractor Address: 6475 City West Parkway
Minneapolis, MN 55344

## Table of Contents



## 1.0 EXECUTIVE SUMMARY

Third Wave Systems (TWS) completed a project funded by the Aviation Development Directorate (ADD) to minimize distortion in an aluminum fatigue coupon machining process. To achieve the objective of this project, TWS utilized its Production Module NC toolpath optimization, AdvantEdge finite element modeling, and distortion modeling software packages. Efforts in Production Module consisted of setting up an analysis of cutting forces across the fatigue coupon toolpath and optimizing these forces to level cutting loads and reduce force spikes. AdvantEdge was utilized to perform detailed finite element simulations of the finish machining toolpath with a focus on understanding the depth and magnitude of machining induced stresses imparted in the workpiece surface. Efforts in the distortion modeling software focused on simulating final part distortion due to the initial bulk stress in the aluminum stock material. TWS performed experimental tests in house to measure the initial bulk stress profiles that were used in the distortion modeling simulations. The outcome of this project was delivery of an optimized NC toolpath that reflected the modeling efforts to minimize final part distortion.

## 2.0 TASK SUMMARY

### 2.1 Task 1: Collect Details of Machining Lab to Support Analysis

The first task of this project was to gather machining process data for the aluminum fatigue coupon to enable simulation and analysis using TWS' Production Module, AdvantEdge FEM and Distortion Modeling products. AAD provided machining process data in the form of NC toolpaths, a cutting tool list as well as material type and dimensions. Data provided by AAD to TWS is listed below:

- Final part solid model
  - MultiBay_V12 Assembly.STEP
- NC toolpaths
  - MultiBay_Side1_profit_Mill.txt
  - MultiBay_Side2_profit_Mill.txt
- NC process data
  - MultiBay_Side1_profit_Mill_Report.xlsx
  - MultiBay_Side2_profit_Mill_Report.xlsx
- Cutting tool list and stock dimensions
  - 403318-01 Tool List – Copy.xlsx

## 2.2 Task 2: Process Modeling and Analysis using Production Module

Utilizing the data gathered in Task 1, TWS created a simulation model of the aluminum fatigue coupon machining process in Production Module. After the input data was loaded into Production Module, a cutting force simulation was performed which provided detailed information on cutting tool forces and process parameters across the NC toolpath. TWS generated an optimized NC toolpath with a focus on leveling cutting loads and reducing force spikes in pocket corners. A top level schematic of the Production Module analysis and optimization process is shown in Figure 2.

Production Module Setup

Defining the machine and controller settings was the first step in the setup of the aluminum fatigue coupon machining process in Production Module. In the machine setup window, Toolpath Type was set to G-code and all controller settings were left at default values. The next step was to define all of the cutting tools used in the machining process. Figure 1 shows the tool setup interface where geometric tool parameters are entered, including diameter, number of flutes, and rake/relief/helix angles. Each tool in the machining process (from 403318-01 Tool List – Copy.xlsx) was set up in Production Module.

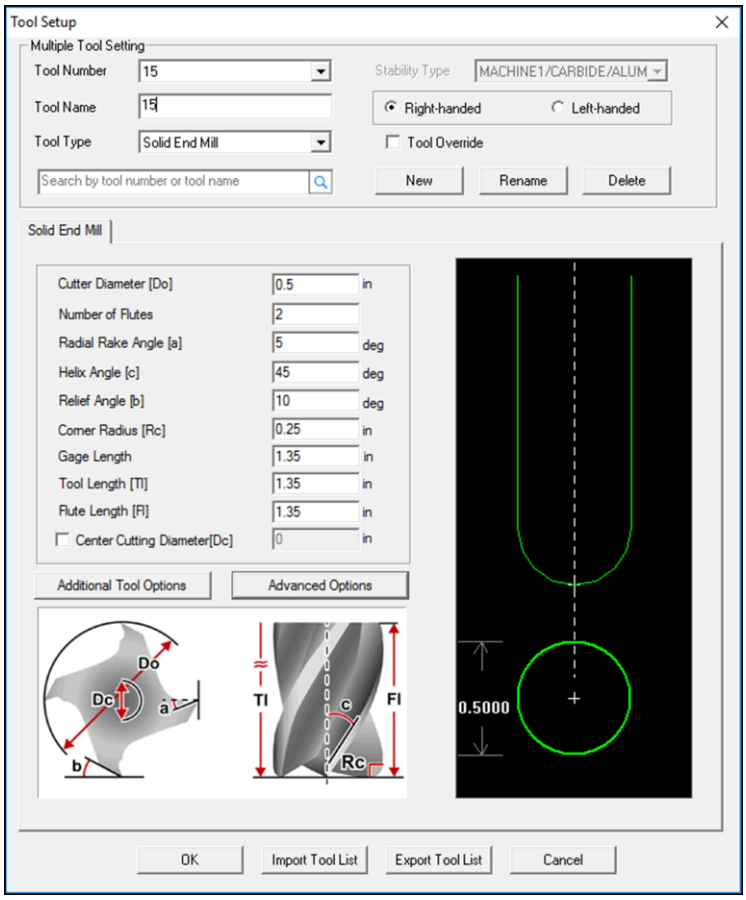


Figure 1. Production Module tool setup window showing tool 15 from the first side machining operation.

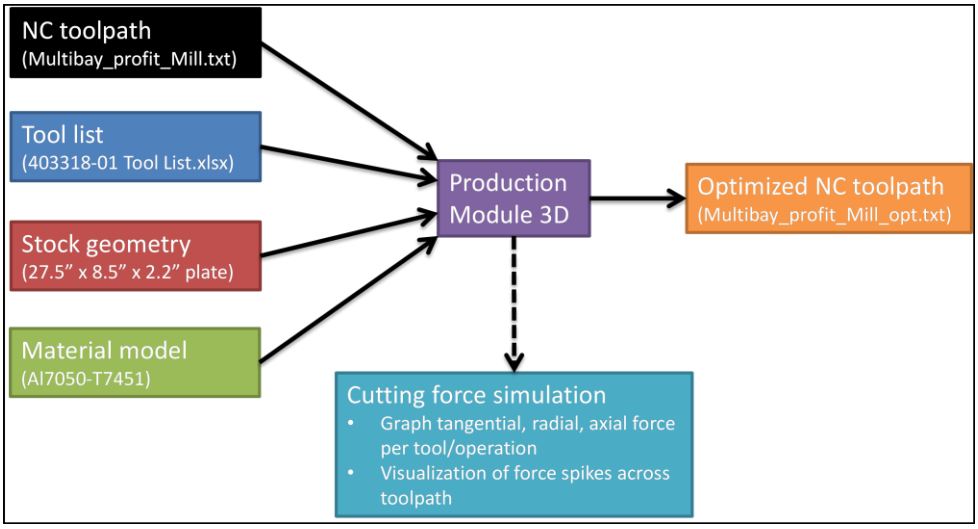


Figure 2. Schematic of Production Module analysis and optimization process

As shown in Figure 3, the workpiece setup window was used to create a model of the starting stock with dimensions of 27.5 inch x 8.5 inch x 2.2 inch. The incoming stock is 2.5 inches but is faced down to 2.2 inches on the machine with a canned cycle operation. Workpiece material model was specified as Aluminum 7050-T7451 from the standard material model database in Production Module. The material model and cutting tool geometry specified in Production Module effect the accuracy of the predicted cutting forces for a machining process analysis.

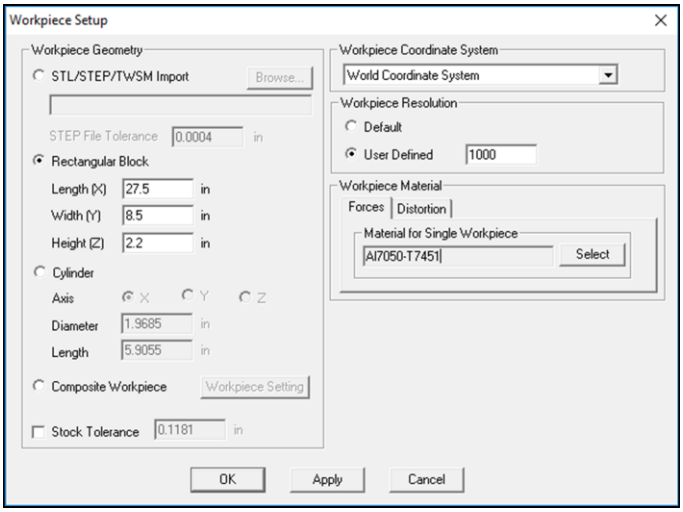


Figure 3. Production Module workpiece setup window showing stock dimensions and material type.

The final step in the Production Module setup was importing the toolpath. The toolpath setup window allows a file of any type to be loaded into Production Module and read as the NC toolpath for the project. Figure 4 shows the toolpath setup window with the NC toolpath for side 1 of the fatigue coupon imported to Production Module.

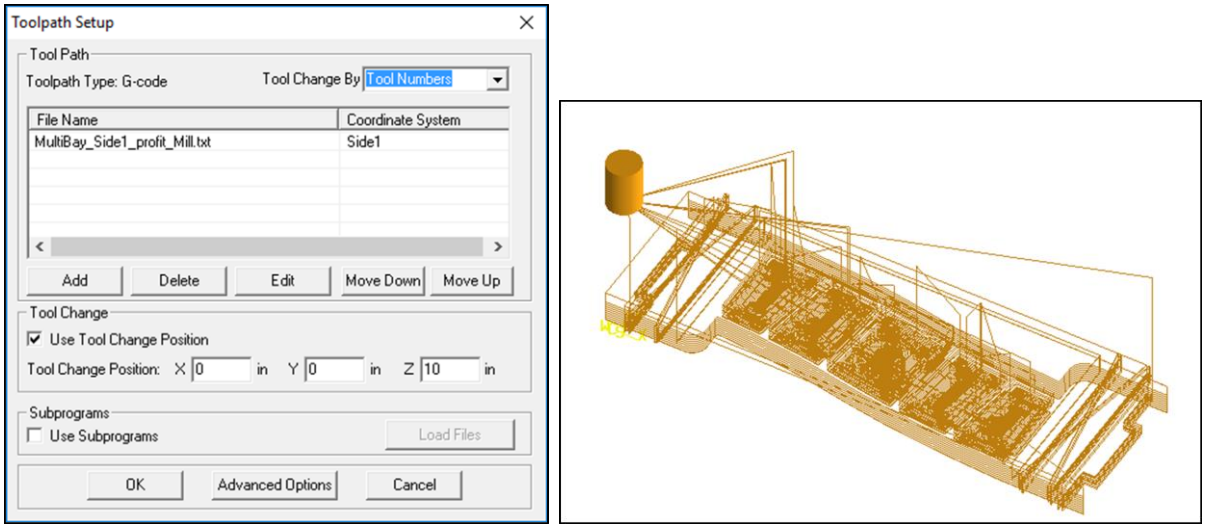


Figure 4. Toolpath setup window (left) and imported toolpath shown in Production Module (right)

## Cutting Force Simulation

With all input data specified in Production Module, a simulation of cutting forces was performed. Several components of cutting force (tangential, axial, radial) as well as detailed chip geometry information is computed by Production Module for every revolution of the cutting tool across the NC toolpath. The force simulation took approximately 20 minutes wall clock time for each side of the aluminum fatigue coupon machining process. Outputs of the cutting force simulation are interactive graph results and visualization of the three dimensional in-process cut stock. Figure 5 shows the three dimensional in process cut stock following the side one machining operation. Figure 6 shows the tangential force graph for side one of the fatigue coupon. The force trace shown is for the entire NC toolpath which was simulated at 53.2 minutes cycle time.

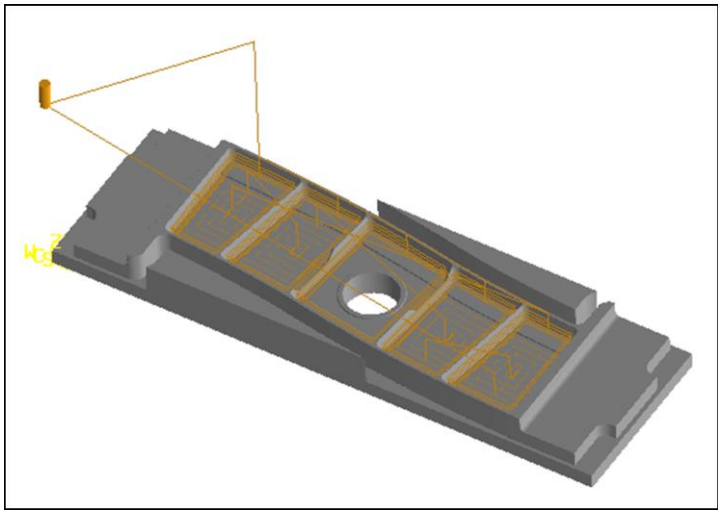

Figure 5. In-process cut stock after machining side one of the fatigue coupon.

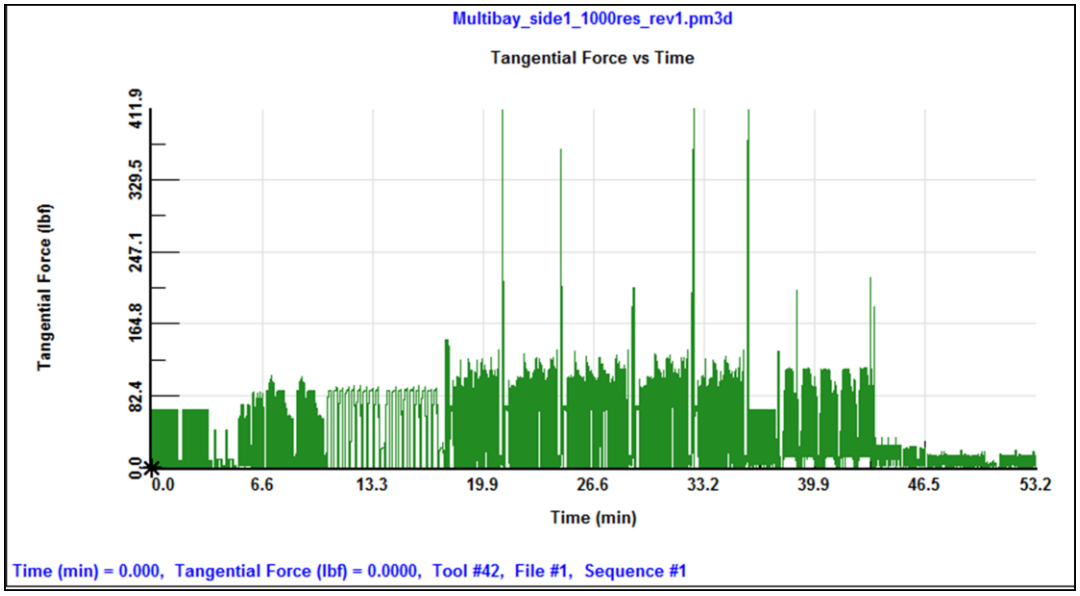


Figure 6. Tangential force graph for side one of the fatigue coupon machining process.

## NC Optimization

The optimization strategy taken in this project focused on minimizing part distortion. To accomplish this, the optimization approach involved leveling cutting forces across the toolpath and reducing force spikes in pocket corners. Figure 7 shows the optimization settings for side two of the fatigue coupon machining process. The left side of the window has a tree listing each sequence (tool) contained in the machining process. Optimization parameters are set in the top right of the window, including primary optimization variable of tangential force, limiting optimization value of load per unit length and maximum in-cut feed

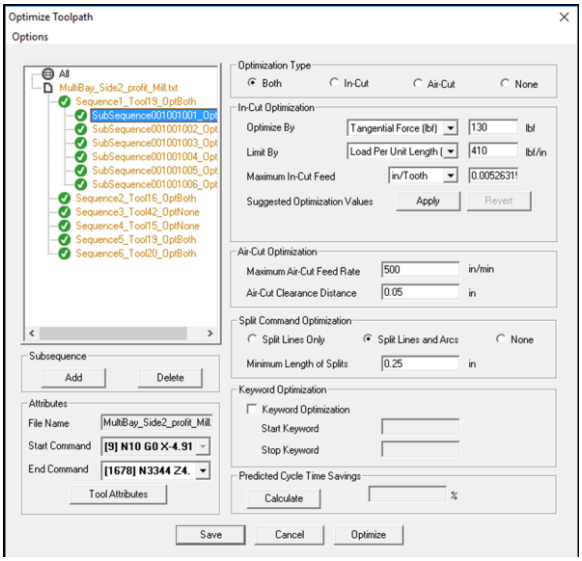


Figure 7. Optimization settings window for side two of the fatigue coupon machining process

rate constraint. Force and maximum feed rate parameters were set per tool based on analysis of the cutting force graphs. Figure 9 shows an example of load level selection for tool 19 from the side two fatigue coupon machining process. A force level of 130 lbf was chosen to reduce force spikes seen throughout the toolpath.

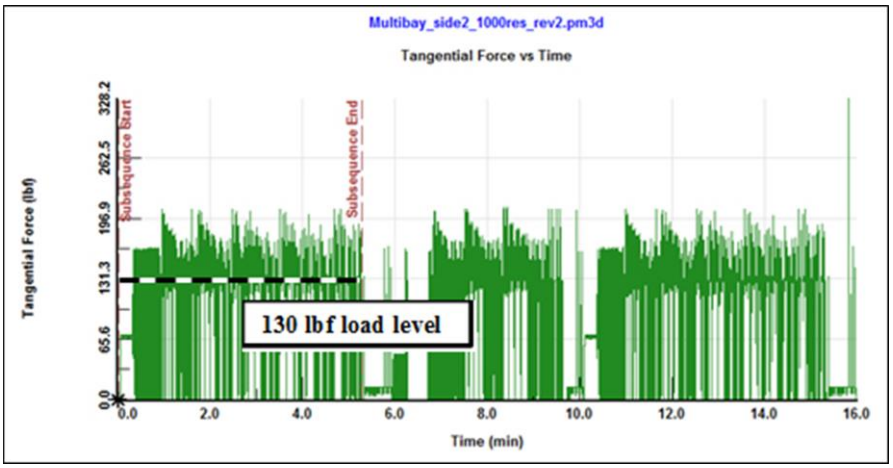


Figure 9. Force graph showing load level selection for tool 19 on the side two machining process

Additional optimization parameters such as maximum air cut feed rate, air cut clearance distance, and split line/arc length are set in this window as well. For both side one and side two of the fatigue coupon all air cut feed rates were set to 500 inch/min, air cut clearance distances set to 0.05 inch and split line/arc length set to 0.25 inch. Optimization results are plotted in Figure 8 for the side one machining process and in Figure 10 for the side two machining process. In each plot, the red force trace is the original toolpath and the green force trace is the optimized toolpath. In both toolpaths, cutting loads have been leveled and force spikes reduced with cycle time lengthened by less than 10 percent.

An additional consideration was taken for the floor finishing toolpath on side two. This operation machines the pocket floors to the final thickness of approximately 0.080 inches and is the most critical machining operation on the part with respect to distortion caused by machining induced stress. A detailed study of this operation is discussed in Task 5 of this report. Using the machining induced stress calculations from Task 5, TWS modified the Production Module optimization parameters for this section of toolpath using the subsequence optimization capability (Figure 11). This feature allows the user to assign different optimization parameters in specific areas of a single sequence. A common application of

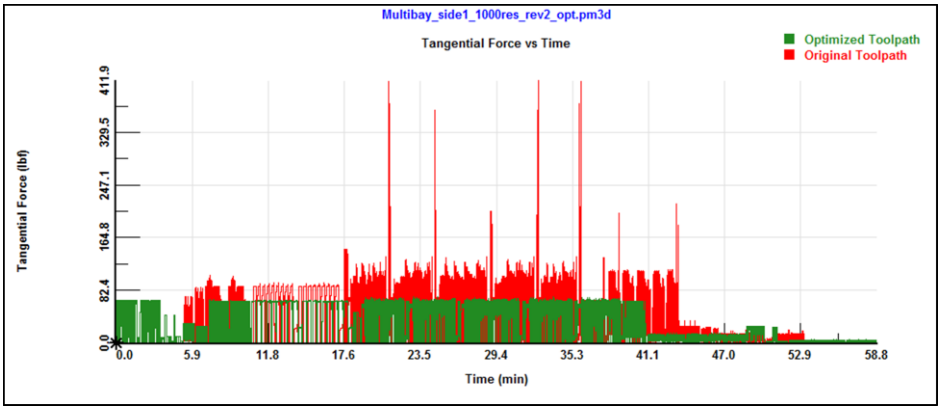


Figure 8. Overlay graph of the original and optimized force profile for side one of the fatigue coupon machining process.

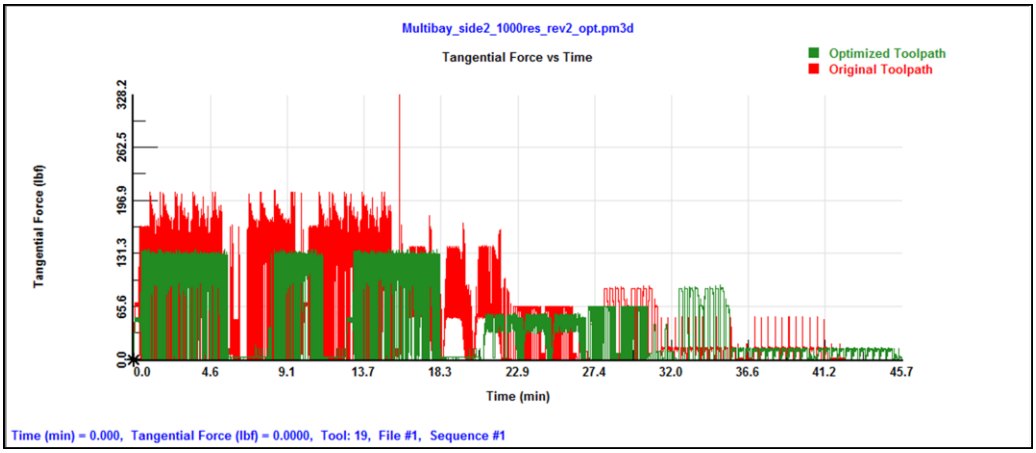


Figure 10. Overlay graph of the original and optimized force profile for side two of the fatigue coupon machining process.

this feature is optimization of a single tool that is performing both roughing and finishing in a single sequence. The user specifies subsequence boundaries by assigning start and end line numbers from the toolpath. For the pocket finishing operations on side two, six subsequences were set. Maximum in-cut feed rate was limited to 0.001 inch per tooth for the finishing operations based on the machining induced

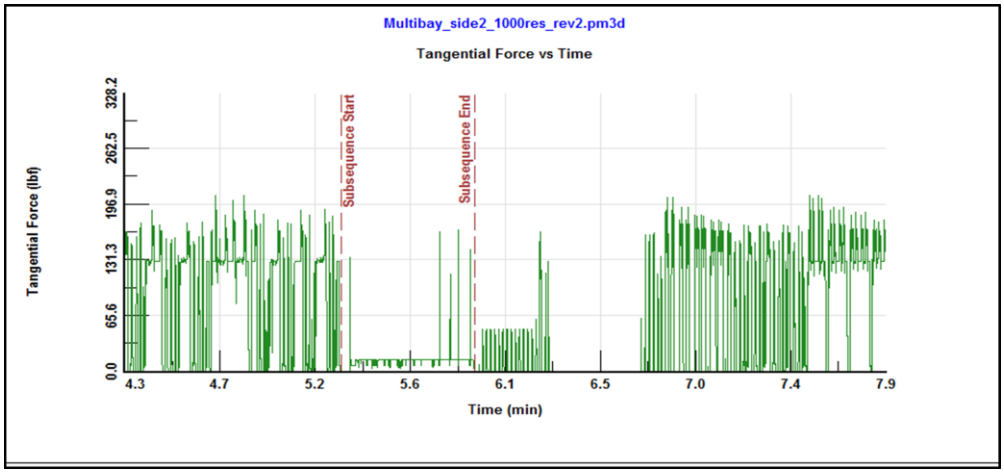


Figure 11. Subsequence optimization of a pocket floor finishing operation on side two. Maximum feed rate was set to 0.001 inch per tooth in these areas based on results from Task 5.

stress simulations from Task 5.

## 2.3 Task 3: Measure Bulk Residual Stress from Material Sample

The objective of Task 3 is to perform laboratory measurements to quantify the bulk residual stress profile in the rolled Al7050-T7451 plate material used to machine the fatigue coupon. A physical plate sample of 12 inch x 12 inch x 2.5 inch dimensions was provided to TWS by AAD. TWS' measurement technique involved machining away layers of material with a slitting saw while collecting strain data with strain gages mounted near the cut.

Figure 12 shows the experimental setup for the bulk residual stress measurements on TWS' Mori Seiki NH6300 machine tool. Strain gages were mounted on top and bottom of the aluminum plate and were

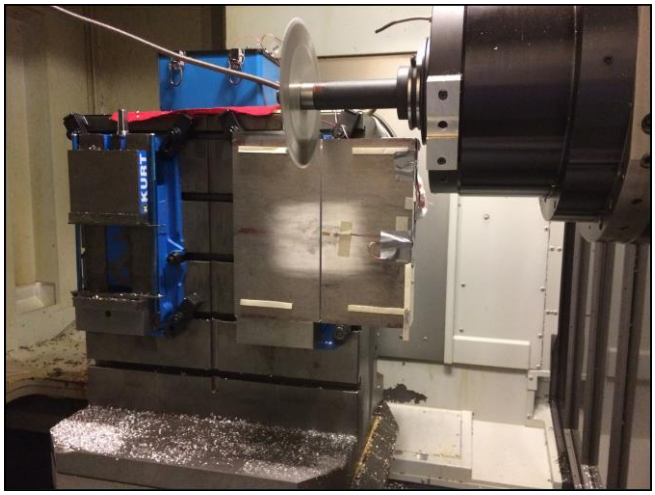


Figure 12. Experimental setup for bulk residual stress measurements on TWS' Mori Seiki NH6300 machine tool

connected to a data acquisition system to record the changing strain on each gage during the test. An 8 inch diameter slitting saw with 0.125 inch thickness was used to perform the machining, with layer depth increments of 0.0787 inches through the plate thickness. Measurements were performed across both the longitudinal and long transverse directions of the plate. The longitudinal direction corresponds to the rolling direction and long transverse corresponds to the perpendicular to rolling direction of the plate.

The raw strain data was reduced using FORTRAN and MATLAB scripts to generate bulk stress profiles in both longitudinal and long transverse directions. The longitudinal bulk stress profile is shown in Figure 13 and the long transverse bulk stress profile is shown in Figure 14. X-axis depth begins at zero (top of plate) and goes through the thickness of the plate to approximately 60 mm. Stress magnitudes fall between positive and negative 20 MPa and the profiles are nearly symmetrical across the midpoint of the plate depth (approximately 30 mm). The symmetric stress profile is a result of the plate rolling process during material manufacture and is a desirable characteristic of T7451 plate. Another interesting

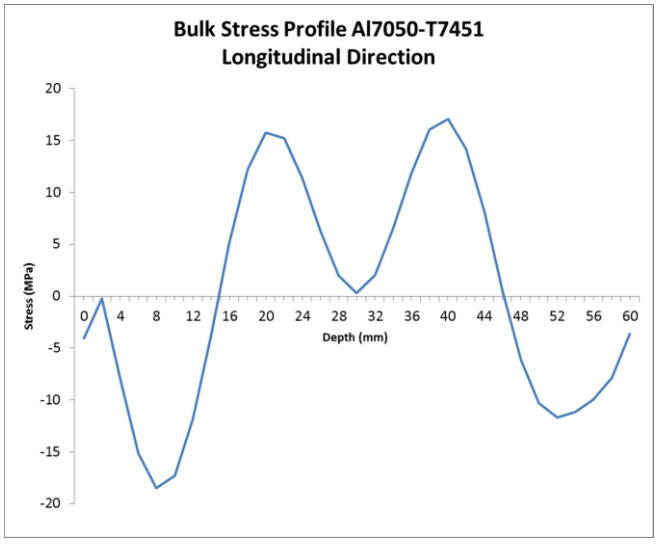


Figure 13. Measured Al7050-T7451 bulk stress profile in the longitudinal direction

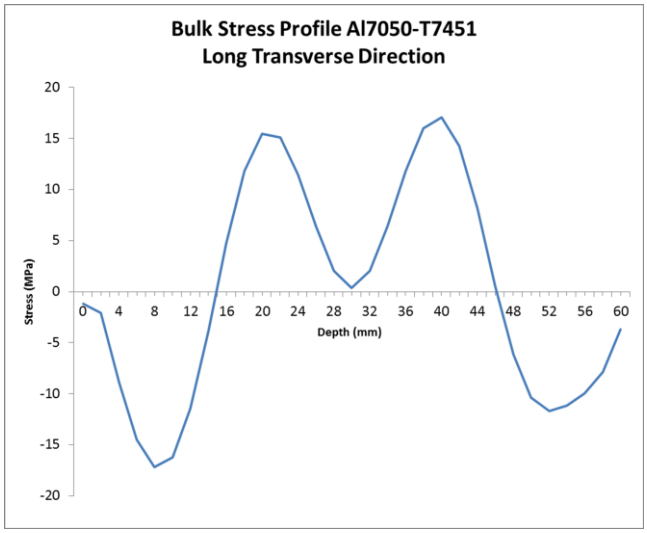


Figure 14. Measured Al7050-T7451 bulk stress profile in the long transverse direction

observation is that the longitudinal and long transverse stress profiles are nearly identical in both magnitude and shape, as can be seen in Figure 15. This is again a desirable characteristic for the plate material.

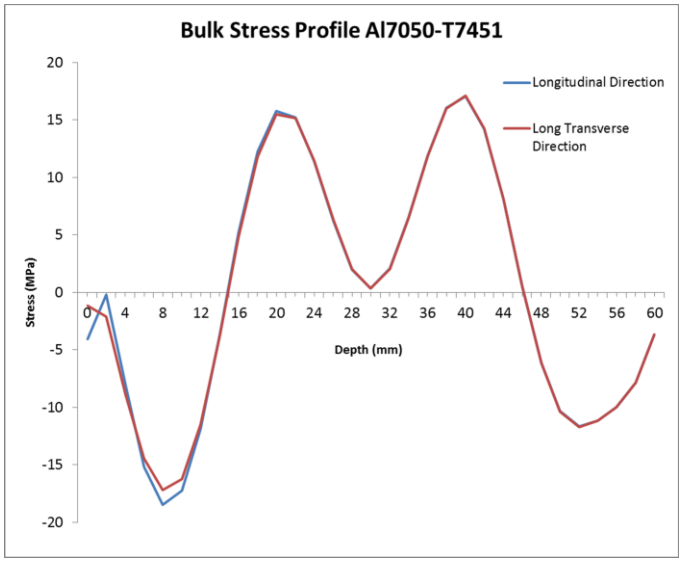


Figure 15. Plot overlaying the measured longitudinal and long transverse stress profiles

## 2.4 Task 4: Part Distortion Prediction and Analysis – Bulk Stress

The objective of Task 4 is to utilize the bulk stress profiles measured in Task 3 to simulate distortion of the finished fatigue coupon geometry. Longitudinal and long transverse bulk stress profiles were loaded into TWS' distortion modeling software as shown in Figure 16 (right). The final part geometry model was also loaded into the distortion modeling software as shown in Figure 16 (left).

With these inputs specified, TWS ran the distortion analysis. Stresses were mapped to the finished part geometry and a solver performed a calculation of resulting part distortion in a three dimensional plot. As

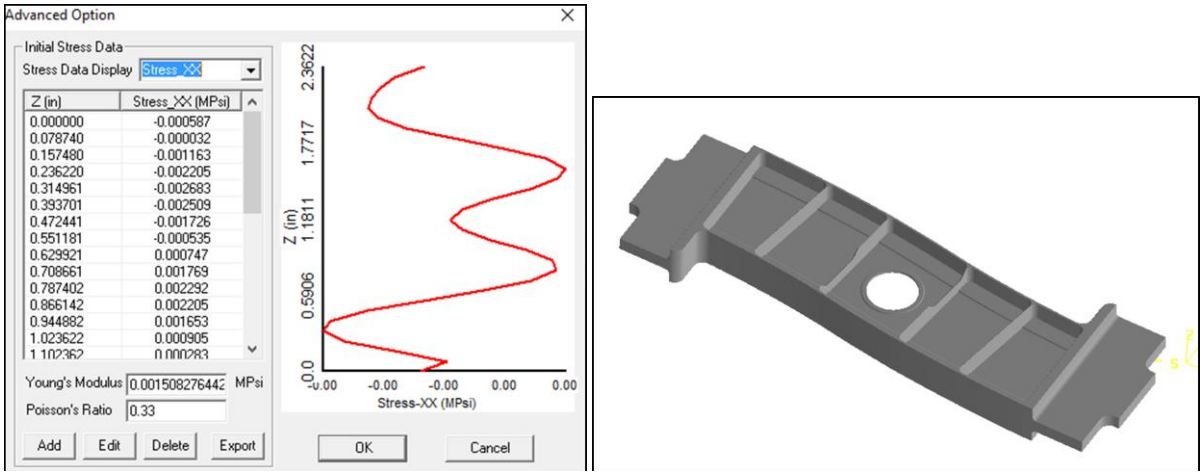


Figure 16. AAD's Al7050-T7451 bulk stress file loaded into distortion modeling software as a custom stress profile (left). Final part model fatigue coupon (right).

shown in Figure 17, this plot contains a three dimensional contour map of distortion magnitude across the final part surface. As seen in the plot legend (lower right of Figure 17 distortion magnitude is visualized on a color scale with blue being zero and red being maximum. The maximum distortion magnitude predicted by TWS' distortion modeling software is 0.0013 inches. A closer inspection of the raised boss around the center hole is shown Figure 18. The probe point shown in the figure indicates a maximum distortion magnitude of 0.00125 inches at this point. The primary conclusion from this task is that bulk

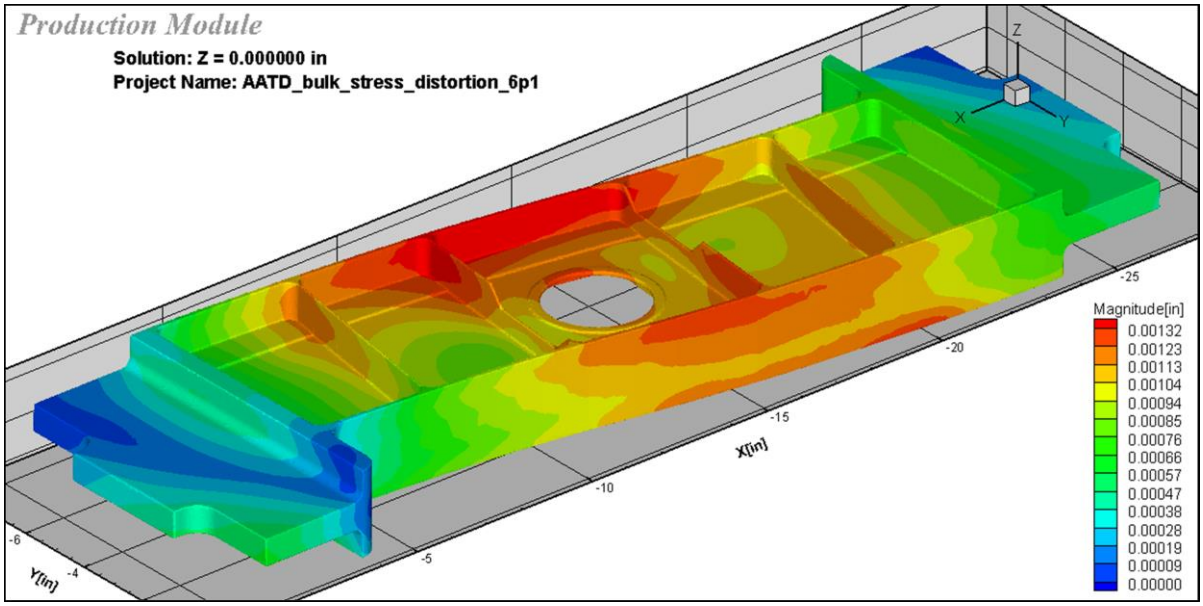


Figure 17. Distortion magnitude prediction for aluminum fatigue coupon. Maximum distortion from bulk stress is approximately 0.0013 inches (red color on contour).

stress from the plate material is well controlled and has a minimal impact on final part distortion.

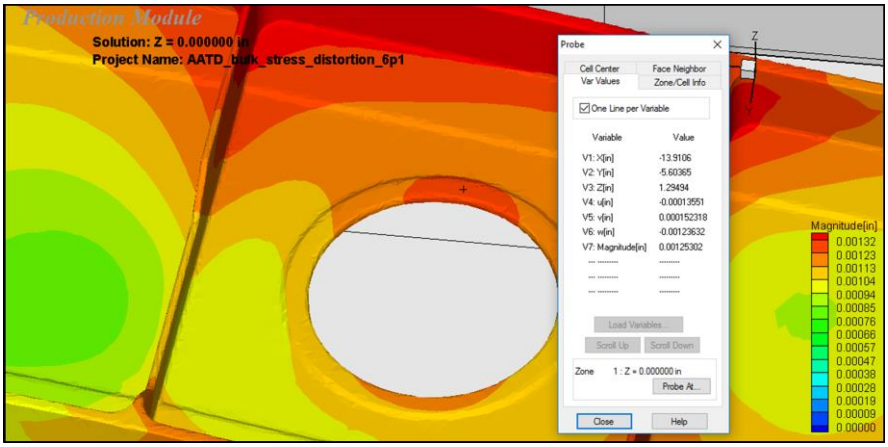


Figure 18. Probe point along circular boss showing distortion magnitude of 0.00125 inches at this location

## 2.5 Task 5: Machining Induced Residual Stress Analysis

Introduction

The goal of this task is to establish the residual stresses left on the workpiece due to the machining process. The location of interest for residual stress analysis on the coupon is first established. Tooling and process conditions that are involved in the creation of geometry at this location are then identified. Tooling geometry information that is critical to the machining process is obtained from tool measurements with an optical microscope. The machining process conditions that are involved in the geometry creation at the location of interest constitute the Baseline Process Condition. This baseline condition is obtained from the optimized tool path information of Production Module software. With respect to the baseline condition's feed and speed, higher and lower values of feed and speed are chosen to construct a 2 x 2 DOE resulting in a total of 5 simulations including the baseline condition. Simulations

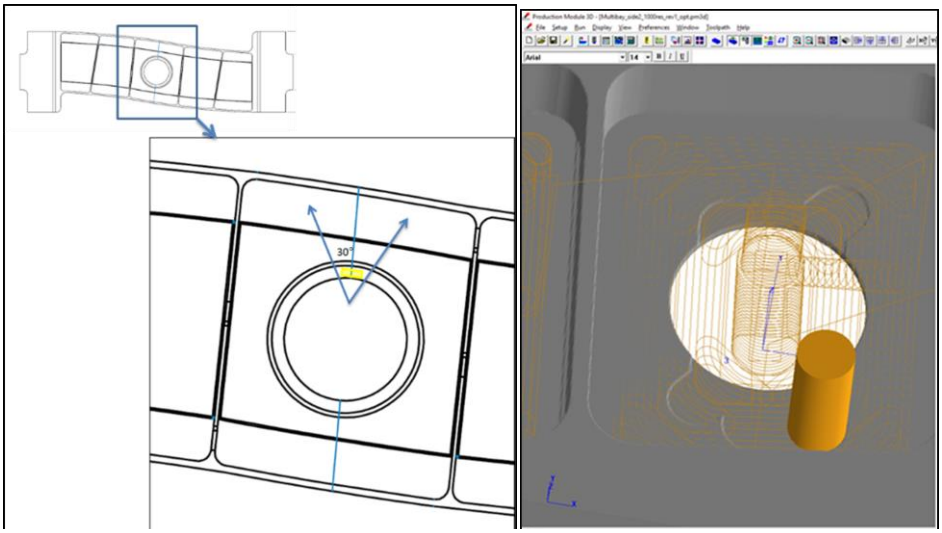


Figure 19. The tool and process details involved in machining this location constitute the Baseline Process Condition. A Production Module image of the baseline machining process is shown above on the right.

are run in AdvantEdge 2D software and the residual stresses from the workpiece surface are extracted and plotted.

Coupon Location for Residual Stress Extraction

The location of interest for studying is highlighted in yellow in Figure 19 the left below. This is the region on top of the boss around the hole. The selection of this region for study is based on previous studies which have indicated this as a critical location for the nucleation and propagation of fatigue cracks. The tool and process details involved in machining this location constitute the Baseline Process Condition.

The tool used in the process is a three-flute end mill of diameter 19.05 mm. The geometry details of the tool cutting edge are obtained as follows. Using commercially available putty, a reverse cast of the tool cutting edge is obtained. This reverse cast is then sliced and studied under an optical microscope. The following tool geometry details are essential for conducting an AdvantEdge 2D simulation: Edge Radius, Rake Angle and Relief Angle. The measurement of these parameters is shown in Figure 20. The tool is made of tungsten carbide and coated with a Z-plus proprietary coating. Although AdvantEdge can account for the addition of a coating layer on the carbide substrate, an uncoated carbide material is used in the simulations. This is because the properties of the Z-plus coating are not available. Additionally, the role of a coating is to typically act as a thermal barrier between the tool and the workpiece and this should have a minimal effect on the residual stresses imparted on the machined workpiece surface.

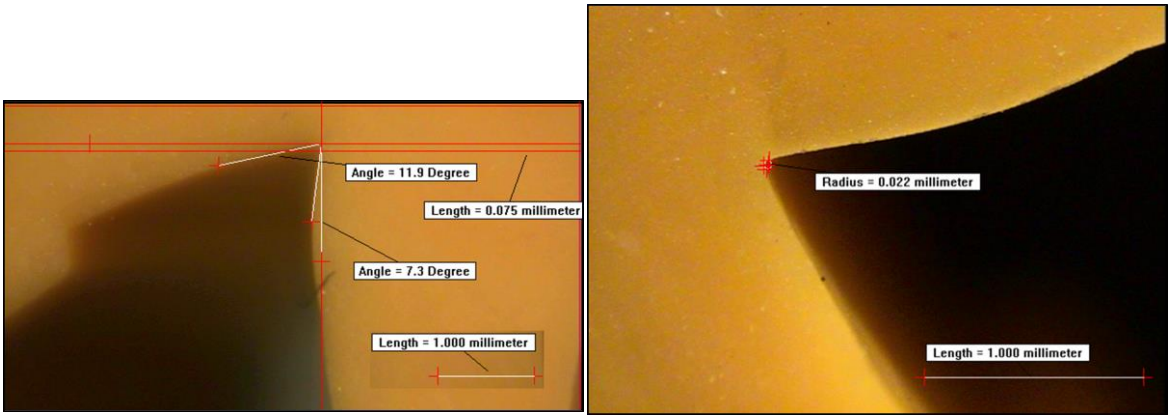


Figure 20. The workpiece material used in simulations is Al7050-T7451

Approximation to 2D

The 3D milling problem is approximated to a 2D problem in the following manner. For a given set of process conditions, the tool encounters a certain chip load at the cutting edge. This is shown in the Figure 21 on the left for a generic three fluted end mill engaged in a finishing operation. The chip load is the resistance magnitude which is measured at the cutting edge in a plane perpendicular to the axis of the tool. For the current milling operation, the baseline condition's Axial Depth of Cut is 0.508 mm and the tool corner radius is 0.02 mm. Therefore, in this case, the chip load describes the tool resistance very close to the floor of the part and therefore will have a pronounced effect on the residual stresses left on the part. This chip load magnitude is then used in a 2D orthogonal setting as shown in Figure 21 on the right, to simulate residual stresses on the workpiece surface. The 2D orthogonal turning simulation assumes a constant chip load unlike a milling simulation where the chip load varies with length of cut. Therefore, the 2D orthogonal setup is based on predicting the maximum residual stresses left in the workpiece which in turn is due to the maximum chip load during a length of cut. An advantage of using 2D in predicting the residual stresses is that a high degree of mesh refinement can be used in a 2D simulation unlike a 3D

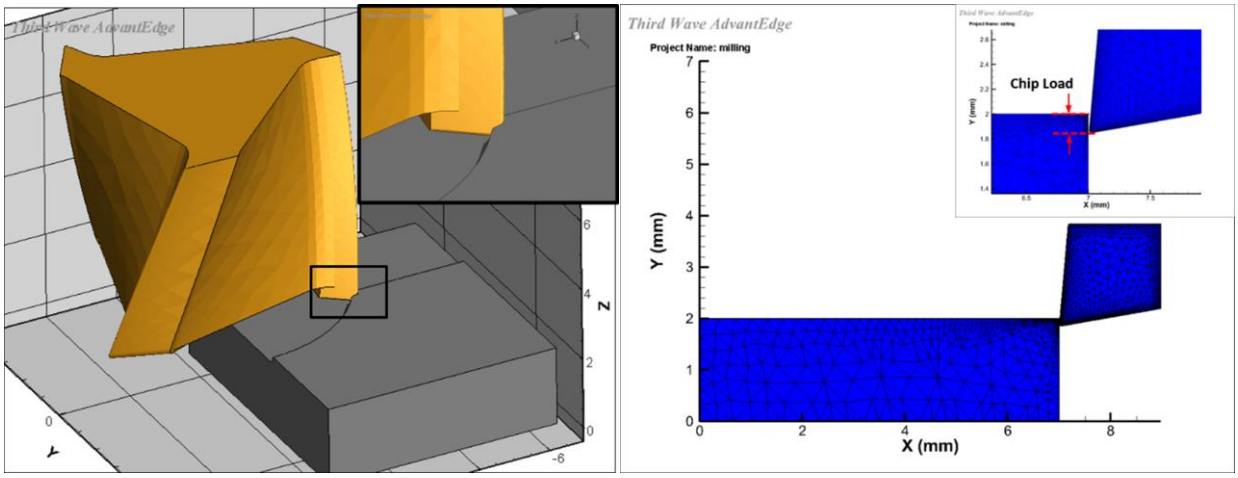


Figure 21. Left: A generic three fluted end mill engaged in a finishing operation. Right: Chip load magnitude used in a 2D orthogonal setting.

simulation where the problem size may quickly grow to cause the simulation to be impractical from a simulation time standpoint.

DOE Approach

The critical process parameters whose influence on the residual stresses left on the workpiece is to be studied are Feed Rate and Cutting RPM. To examine the sensitivity of the critical parameters on the residual stresses left on the workpiece a 2 x 2 DOE is constructed in the following manner. With respect to the baseline condition's value of each critical parameter, a value higher and lower than the baseline value is chosen. Combinations of the HIGH and the LOW values for each of the two critical parameters are taken resulting in a total of 4 combinations. This results in a total of 5 simulations when the baseline condition is included with these combinations. The results from this DOE can now be used in comparing the change in residual stress results from the baseline condition to any of the other conditions. The final list of process conditions is shown in Table 1.

Table 1: Process conditions for machining induced stress finite element simulations

| S.No. | TYPE | Chip Load (mm/tooth) | Cutting Speed (m/min) |
|---|---|---|---|
| 1 | Baseline | 0.0762 | 568 |
| 2 | High Feed – High Speed | 0.127 | 671 |
| 3 | High Feed – Low Speed | 0.127 | 427 |
| 4 | Low Feed – High Speed | 0.0254 | 671 |
| 5 | Low Feed – Low Speed | 0.0254 | 427 |

Residual Stress Extraction

Residual stress machining simulations are run using the orthogonal turning setup described earlier. As seen from in Figure 22 on the left, a high level of mesh refinement is retained on the workpiece during and after cutting. This helps obtain highly accurate stress contours on the workpiece.

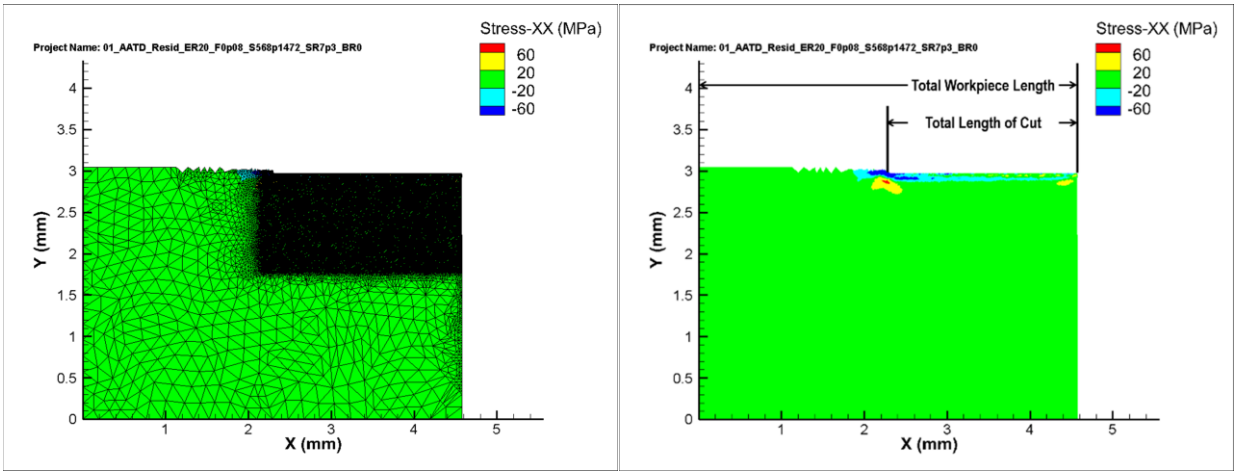


Figure 22. High levels of mesh refinement are retained on the workpiece during and after cutting

The procedure for residual stress extraction is as follows:

- A fixed location is chosen, as a percentage of the total Length of Cut (LOC) (Figure 22 on the right) on the workpiece based on the following considerations
  - » Steady State - The LOC for residual stress extraction must be greater than the minimum length of cut necessary for the forces and temperatures to achieve a steady state i.e. constant with respect to time in the simulation.
  - » End Effects – The start of the workpiece represents a freely deformable boundary and the extraction LOC must be sufficiently far away from the starting point of the LOC.

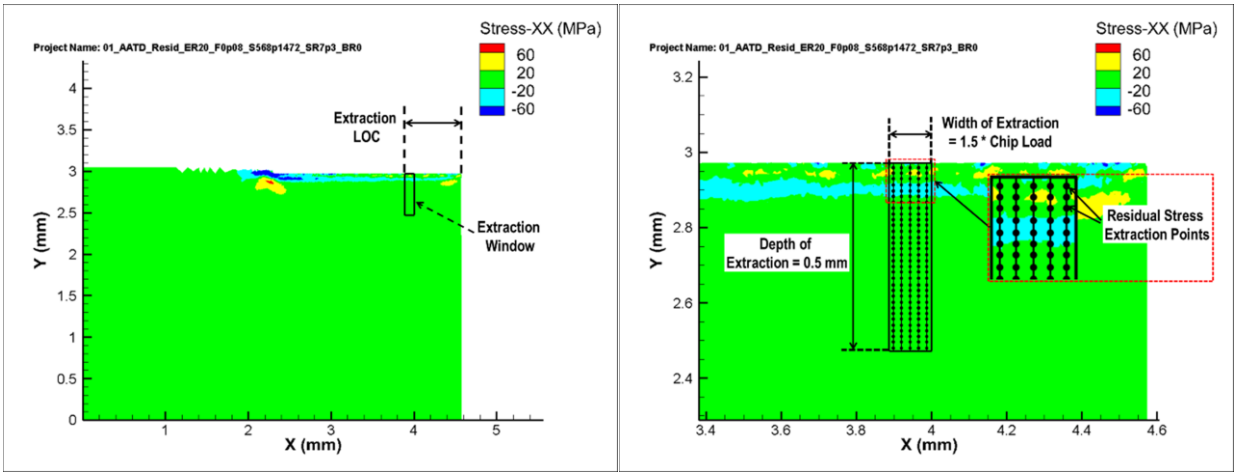


Figure 23. Stress extraction taken at 30% of LOC (left). Extraction averaging window (right).

  - » Based on the above factors, the extraction LOC is chosen as 30% of the total length of cut and this is shown in Figure 23, on the left. This condition satisfies either of the conditions mentioned above.
- Starting at the extraction LOC, a window is defined in the workpiece inside which residual stresses are to be extracted along lines, as shown in Figure 23 on the right.
  - » The width of the extraction window is chosen to be 1.5 times the chip load to provide the necessary and sufficient region over which to average residual stresses.
  - » The depth of extraction is chosen as 0.5 mm. This depth is sufficient to capture the residual stress below the surface to the depth where it becomes zero or very close to zero. This is true for all stress components and all simulation conditions.
  - » Residual stresses are then extracted along multiple lines within the extraction window at equal intervals along the depth of extraction. The number of extraction points along the length of an extraction line is 80. The number of line extractions used within the extraction window is 40. This allows for thoroughly sampling the region within the extraction window.
  - » The residual stresses corresponding to the same height between different extraction lines are averaged to finally obtain a single curve for a stress component versus the depth. The data is averaged over an area rather than extracted from a single line because of the following reason: stress results from explicit finite element simulations such as AdvantEdge FEM encounter some degree of numerical noise that results in local stress oscillations. Although, these oscillations have been kept to a minimum through recommended practices such as mesh refinement, it is not possible to completely avoid them. Averaging allows for suppressing numerical noise so trends that are true can be picked up. This also facilitates comparison of residual stress extractions between different simulations with different process conditions to accurately isolate trends in residual stresses between them.

Residual Stress Results

The residual stress results compared for different conditions for each stress component is presented in this section. Under each stress component's heading, the first plot compares the averaged data for each process condition with the other process conditions. The other plots indicate the variability of the stress component as a function of depth for the different process conditions. Variability about the average is quantified by continuous curves corresponding to Average ± 2 x Standard Deviation. The measure 2 x Standard Deviation is used because if a data set can be approximated as a normal distribution, then 95% of the data will lie within the range Average ± 2 x Standard Deviation.

The influence of the different process parameters on residual stresses is identified using the following phenomena:

- Tensile/Compressive Peak – When measured along the depth into the workpiece surface, the residual stress profile typically exhibits a maximum value in tension before changing to a maximum value in compression and finally reducing to a near zero value, as shown in Figure 24. The maximum values in the tensile and compressive directions are called correspondingly the tensile and compressive peaks.
- Tensile/Compressive Peak Depths – The depth measured into the workpiece at which the tensile and compressive peaks occur.
- Depth of Influence – After exhibiting the tensile and compressive peak, the stress usually reduces to zero or near to a zero value. This depth represents the total depth of influence of the residual stress profile.

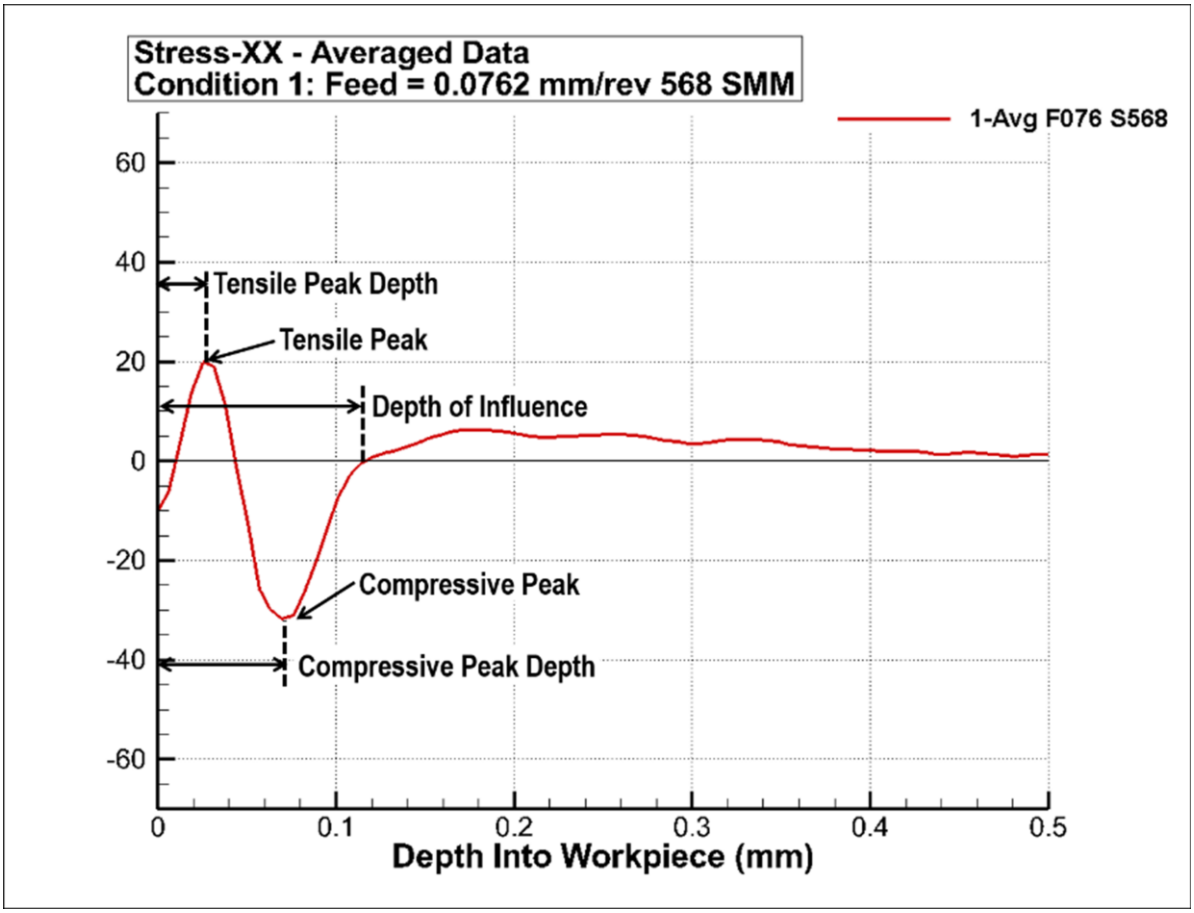


Figure 24. Description of residual stress profile parameters

Stress-XX – Stress Component in the Direction of Cutting

Increasing feed rate and cutting speed from the baseline condition (a) increases the tensile peak value and the tensile peak depth (b) results in a similar compressive peak but increases the compressive peak depth significantly (c) increases the total depth of residual stress influence significantly. Similar trends when compared to the baseline are observed but to a lesser degree when the feed rate is increased but the cutting speed is decreased. This shows feed rate as a dominant factor in influencing Stress-XX residual stress. Decreasing the feed rate and increasing the cutting speed from the baseline condition (a) results in similar tensile peaks as the baseline but a lower tensile peak depth (b) higher compressive peak but shorter compressive peak depth than the baseline. Results for the stress-XX extractions are shown in Figure 25.

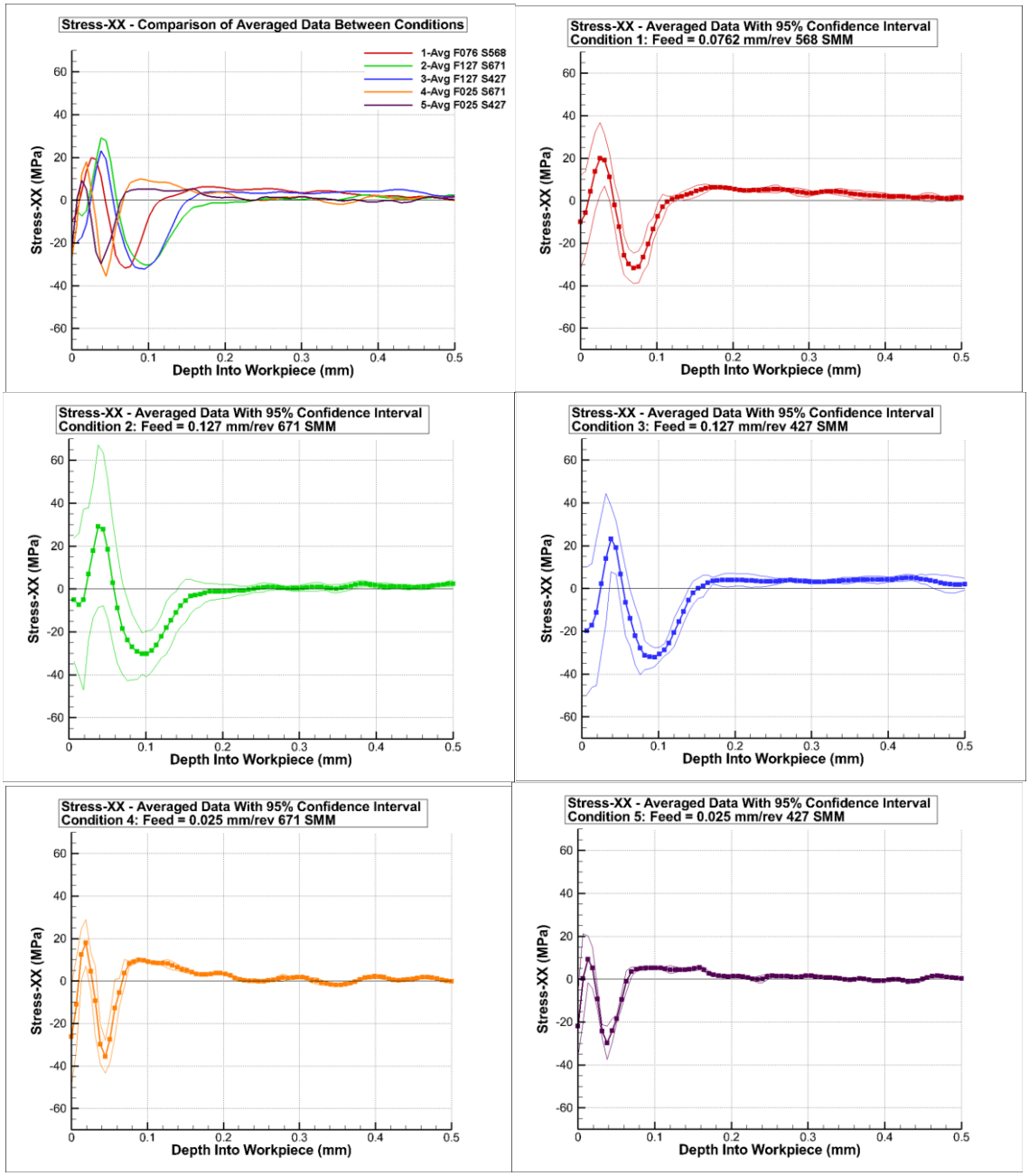


Figure 25. Results for stress-XX, stress component in the direction of cutting.

Decreasing the feed rate and cutting speed from the baseline condition results in a (a) significantly lower tensile peak and tensile peak depth than the baseline (b) similar compressive peak but significantly lower compressive peak depth than the baseline (c) significantly lower depth of residual stress influence than the baseline. These results clearly show that the depth of tensile and compressive peaks follows the trend of increasing or decreasing feed rate.

Stress-YY – Stress Component Normal to Direction of Cutting in Direction of Feed

As seen from the stress variability graphs in Figure 26, the stress-YY component exhibited symmetric variation about the X-axis for conditions 1, 2 and 3 at all depths resulting in a near zero residual stress state when averaged. Considering only the positive limits of the confidence intervals for conditions 1, 2 and 3 shows the tendency for the tensile peak and its depth to follow the trend of increasing/decreasing

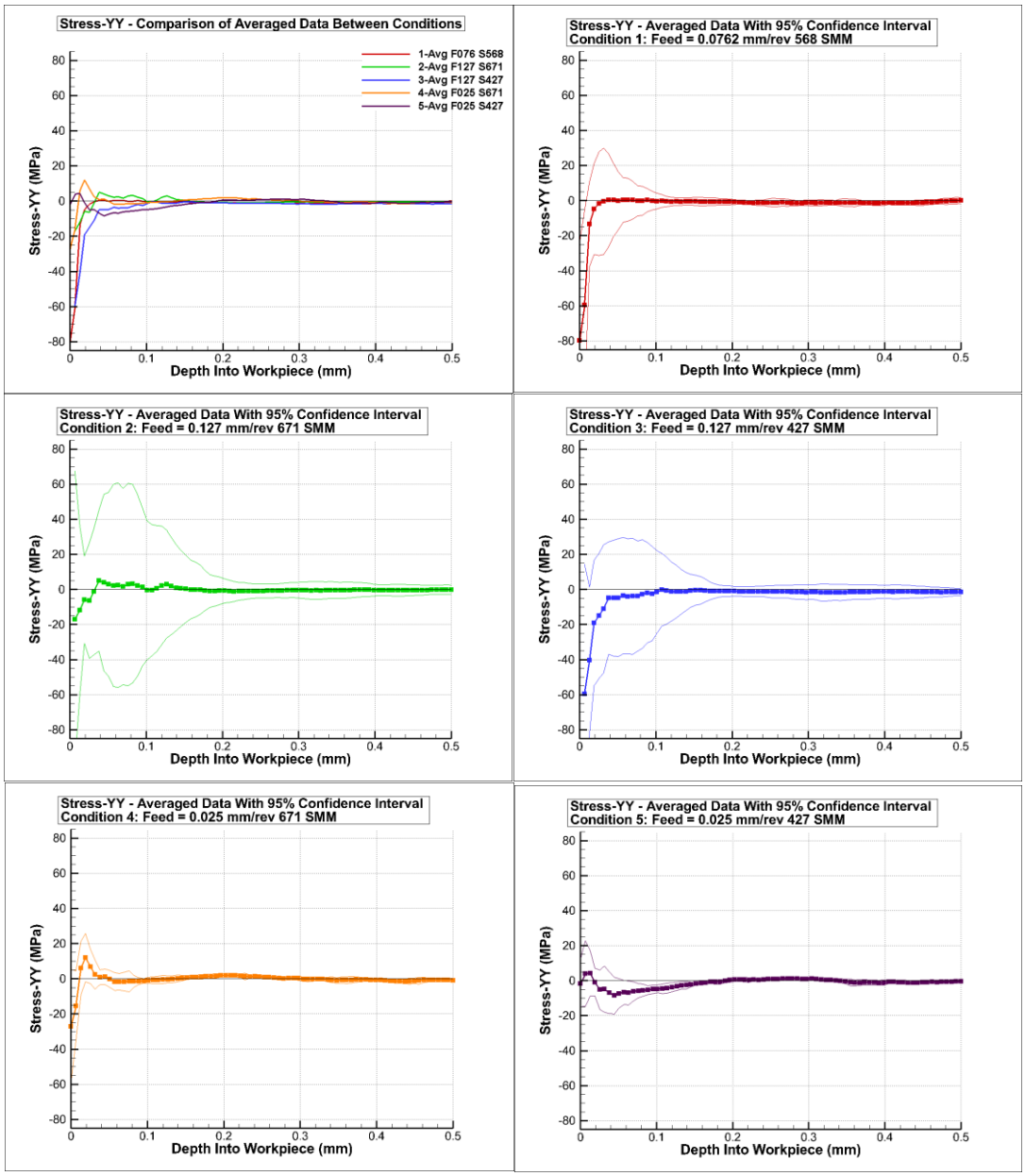


Figure 26. Results from stress-YY, stress component normal to direction of cutting in direction of feed

feed rate.

The same can be also said of the lower confidence limit and the compressive peak. Conditions 4 and 5 show lower variability compared to conditions 1, 2 and 3 showing that the trends exhibited are true.

Conditions 4 and 5 exhibited the tendency to form tensile and compressive peaks but the stress magnitudes at any point along the depth are not significant.

Stress-XY

The shear stress exhibited similar trends to stress-YY, as shown in Figure 27. The stress-XY component exhibited a symmetric variation about the X-axis for conditions 1, 2 and 3 at all depths resulting in a near zero residual stress state when averaged. Conditions 4 and 5 show lower variability compared to conditions 1, 2 and 3 showing that the trends exhibited are true. However, for these conditions the stress magnitudes at any point along the depth is not significant.

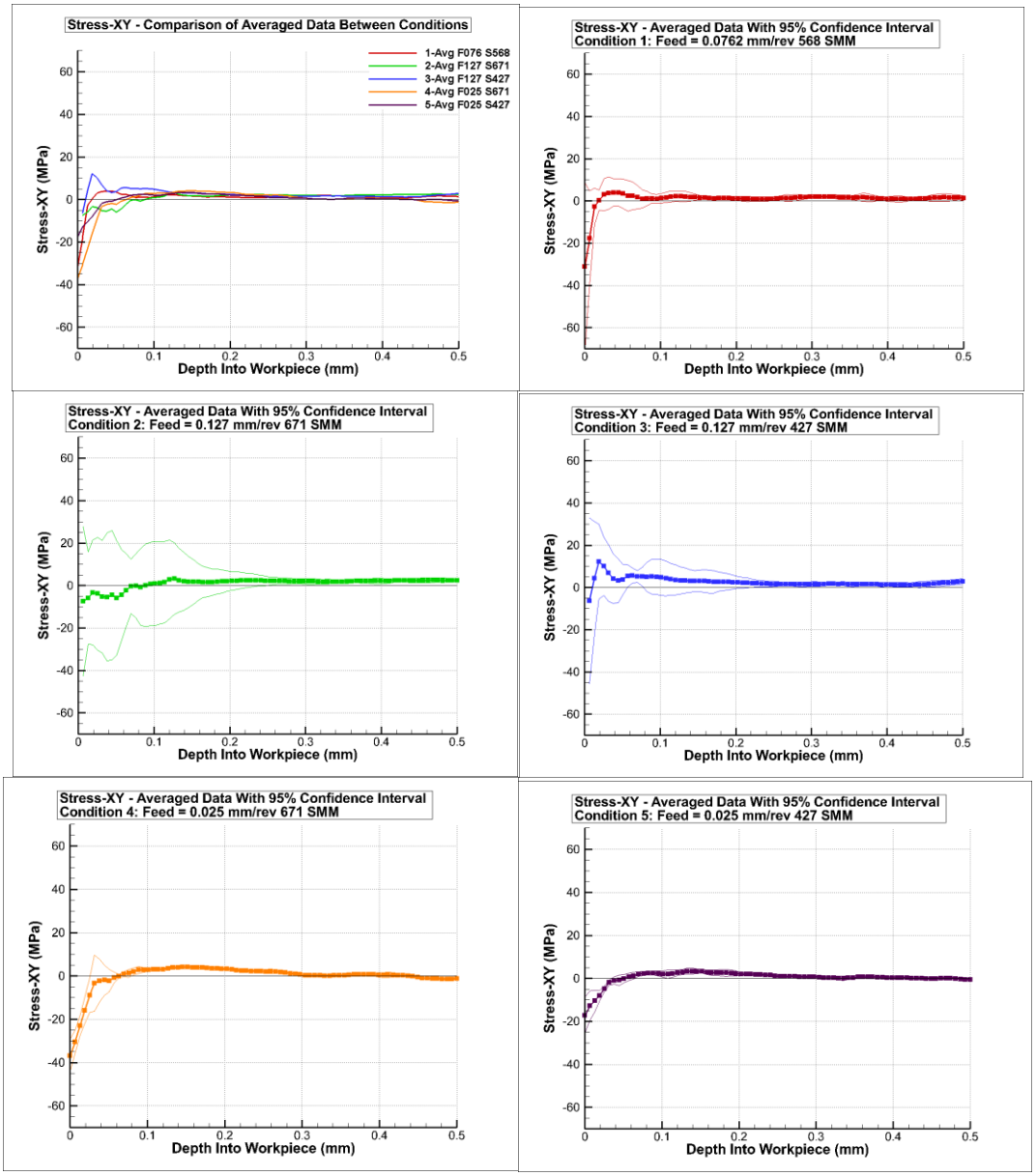


Figure 27. Results for Stress-XY, shear direction.